

Remote Sensing in OMEX II-II

Peter Miller, Steve Groom, Tim Smyth and Monica Miguel-Lago

Remote Sensing Group - Centre for Coastal and Marine Science - Plymouth Marine Laboratory
Prospect Place, West Hoe, Plymouth PL1 3DH, United Kingdom - E-mail: PIM@ccms.ac.uk

Abstract

The past year has seen the most intense remote sensing activity in OMEX to date; the undoubted highlight being the *Charles Darwin CD114* cruise in August 1998. The provision of *sea-truth* biological measurements during last summer's cruises provided considerable impetus to the improvement, research and development of SeaWiFS algorithms. These algorithms attempt to relate the radiance measured by SeaWiFS to various biological parameters such as chlorophyll *a* concentration and phytoplankton primary production. Optical measurements aboard the *Belgica BG9815* cruise using a radiometer rig operating at the same wavelengths as SeaWiFS, together with *in situ* HPLC derived pigments, allowed validation of SeaWiFS atmospheric correction and chlorophyll *a* algorithms. The relationship between SST and Nitrate has also been investigated, to enable the new fraction of primary production to be determined using remote sensing. On the operational side, approximately 2000 SST maps and 350 ocean colour scenes were processed this year for the OMEX region on the same day as reception, and made available over the World-Wide-Web. In total five OMEX cruises were supported with near-real time imagery. A six-year sequence of composite front maps was compiled to provide optimal visualisation of upwelling and filaments. Statistics have been compiled describing onset, variability and strength of the Galician upwelling for the period 1981 to 1999.

Introduction

This report describes the activities carried out by the CCMS-PML Remote Sensing Group during the second year of the OMEX II-II project on Work Packages I and II. The primary roles of remote sensing within OMEX are: (i) to support cruises by providing real-time information on the location of fronts, upwelling, filaments, and eddies; (ii) to calculate statistics on the distribution and attributes of such features; (iii) to assemble a regional archive of SST and ocean colour data for comparison with *in situ* measurements and model results and (iv) to research ocean colour and temperature algorithms for deriving surface maps of biological parameters, including phytoplankton pigments, primary production, and nutrients.

Methods

Ocean colour

NASA's Sea-viewing Wide Field-of-view Sensor (SeaWiFS) is an optical scanner with 6 channels in the visible spectrum (412, 443, 490, 510, 555, and 670 nm) designed to provide optimal discrimination of phytoplankton, suspended particulate matter and coloured dissolved organic matter. It operates in a sun-synchronous orbit, with all data captured at local noon. The swath is 2800 km wide, and the resolution is 1.1 km at the sub-satellite point. One or two passes over NW Europe are received every day by the Dundee Satellite Receiving Station, and are then immediately transferred to Plymouth via the Internet for processing into calibrated ocean colour products. OMEX *in situ* data have been used in conjunction with SeaWiFS ocean colour data to develop algorithms for retrieval of chlorophyll *a*, phytoplankton primary production and new production.

(i) *Primary production*: During *CD114* a number of primary production variables were taken including 24-hr ¹⁴C incubations, High Precision Liquid Chromatography (HPLC) pigments (including chlorophyll *a*), P-E photosynthesis parameters, in-water irradiance and phytoplankton absorption.

(ii) *Validation of SeaWiFS chlorophyll retrievals*: An OMEX aim in WP II is the validation of the SeaWiFS retrievals of chlorophyll *a*. These have been calculated using the standard NASA OC2 algorithm (with the complete data set undergoing a re-analysis with the new OC2 version 2 algorithm). Excellent weather, in terms of lack of cloud cover, encountered during the *Belgica BG9815* and

Charles Darwin CD114 cruises enabled comparison of SeaWiFS chlorophyll retrievals with *in situ* HPLC chlorophyll taken within either 12 or 2 hours of the satellite overpass.

(iii) *Remote sensing of new production: SST-Nitrate Algorithms*: The Sathyendranath *et al.* (1991) approach to calculating new (or the nitrate driven) fraction of primary production relies on relating surface nitrate concentrations to sea-surface temperature which can be retrieved from satellite. *In situ* data obtained prior to and during OMEX II-II have been gathered to investigate such relationships.

In situ optical measurements

The OMEX Remote Sensing Group is responsible for providing validated SeaWiFS imagery of the region of interest. An important component of the world-wide SeaWiFS project is to provide *in situ* optical and biological measurements to add to the global ocean colour validation database. The OMEX project afforded an excellent opportunity to sample in a region of upwelling characterised by moderate to high chlorophyll *a* concentrations (<7 mg m⁻³), which is currently under-represented in the database. Optical and pigment measurements were taken on board the *BG9815* cruise from 27th June to 7th July 1998.

Optical measurements were taken using a radiometer rig that measured upwelling and downwelling radiance at the same operational wavelengths as SeaWiFS. A deck cell measuring downwelling irradiance was permanently attached to the ship on the sun-deck for normalisation purposes. The rig was lowered into the water at a rate of 25 cm s⁻¹ to a depth of 60-80 m before being raised back to the surface at the same rate. Pigment samples were taken coincidentally with the optical profiles. These were filtered aboard the *Belgica* and then packed in dry ice and flown back to the UK upon the completion of the cruise for HPLC analysis.

SeaWiFS estimates the sea-surface chlorophyll by way of an empirical algorithm that relates radiances measured at several discrete wavelengths to chlorophyll *a*. Therefore, to validate (and hence develop and improve) these algorithms, comparison must be made between (a) the normalised water leaving radiance (L_{wn}) measured by SeaWiFS and that measured by the optical profiler and (b) comparison between HPLC measured concentrations of chlorophyll *a* and that derived via algorithm using the optical profiling rig.

(i) *Water-leaving radiance (L_{wn}) comparison*: The main purpose of comparing the SeaWiFS and optical profiler derived L_{wn} is to check on the validity of the atmospheric correction algorithm used by SeaWiFS. The L_{wn} at each wavelength were derived from the raw profiler and deck cell data using the following method. The sub-surface remote sensing reflectance (R_{rs-0}) was calculated using the equation

$$R_{rs-0} = \frac{L_u(I)}{E_s(I)}$$

where $L_u(\lambda)$ is the upwelling radiance measured by the optical profiler and $E_s(\lambda)$ is the downwelling solar irradiance measured by the deck cell. A linear regression is carried out of the natural-logarithm of R_{rs-0} against depth to calculate the value of R_{rs-0} at the sea surface. The top 1.5 m of data are removed to prevent surface effects such as internally reflected light contributing to the signal; data below 20 m are discarded as the optical signal is relatively weak. The normalised water leaving radiance is then calculated using

$$L_{wn}(I) = R_{rs-0}(I) \times 0.542 \times F_0(I)$$

where $F_0(\lambda)$ is the mean extra-terrestrial solar irradiance and the factor 0.542 accounts for the Fresnel reflectance and change in refractive index across the air-sea interface. The data were quality assured such that all profiles having $r^2 < 98\%$ in the linear regression analysis of natural-log of R_{rs-0} against depth were discarded.

(ii) *Pigment algorithm validation*: In remote sensing another parameter, called the Remote Sensing Reflectance (R_{rs}), is often used. It is defined as:

$$R_{rs}(I) = R_{rs-0}(I) \times 0.542$$

R_{rs} at various wavelengths is commonly used in chlorophyll *a* empirical algorithms. The equation used currently by SeaWiFS (OC2V2) takes the form of:

$$R = \log\left(\frac{R_{rs,490}}{R_{rs,555}}\right), \text{ and } OC2V2 = 10^{(a0+a1 \times R + a2 \times R^2 + a3 \times R^3)} + a4$$

where $a_0 = 0.2974$, $a_1 = -2.2429$, $a_2 = 0.8358$, $a_3 = -0.0077$ and $a_4 = -0.0929$. The efficacy of the algorithm was tested using the values of $R_{rs}(\lambda)$ obtained using the optical rig in the OC2V2 equation and comparing with the *in situ* HPLC measurements of chlorophyll *a*.

Statistical information on physical features

The development of the Panorama automated processing system was described in the previous annual report, and in the literature (Miller *et al.*, 1997; Miller *et al.*, submitted). Panorama automatically generates large data-sets of high-resolution satellite ocean temperature and colour maps, raising practical problems for interpretation by oceanographers, involving laborious visual browsing and analysis to locate and characterise features of interest. An automated front detection algorithm has been added to Panorama, based on one published by Cayula and Cornillon (1992), which detects the subtle differences between neighbouring water masses associated with frontal boundaries on AVHRR SST images. Experiments using SeaWiFS ocean colour data have indicated that the algorithm is equally appropriate for detecting chlorophyll gradients. Partial observations of fronts in a sequence of cloudy scenes are then combined using a compositing technique, which drastically improves the applicability of this method in cloudy conditions. The composite front map provides a powerful synoptic visualisation of surface processes and a detailed time-series of the movement of dynamic features such as fronts, filaments or eddies that would instead be blurred in a composite SST or chlorophyll map. This methodology has proved to be robust enough to apply to 10,000 SST images covering 6 years of the OMEX II-II region, to create 2,000 3-day front maps.

Animated sequences of front maps enable visualisation of dynamic processes such as filament growth and eddy rotation; certain sequences have been made available on the web site for use in describing the physical context of cruise measurements and for validating mesoscale features seen in model runs (<http://www.npm.ac.uk/rsdas/omex/>).

One of the most important statistics to derive for the OMEX box is the seasonal distribution of upwelling and downwelling, as this effects most other physical and biological parameters. A long time-series of upwelling indices for the Vigo region has been obtained from a US National Oceanic and Atmospheric Administration (NOAA) research group. The source data are the FNMOC synoptic pressure fields derived from ship, buoy and modelled data. From these the geostrophic wind vectors are calculated, and then converted into estimates of Ekman offshore transport using Bakun's method (Schwing *et al.*, 1996). The monthly average upwelling indices have been obtained for 42°N, 9°W from 1981 to 1999, and from these the seasonal distribution of upwelling has been derived.

Results

1.1 Near real-time cruise support: Remote sensing support during the 1998 upwelling season has been of crucial importance to the success of several cruises studying the exchange generated by dynamic and transient upwelling filaments. In particular, the Work Package I cruise on *Charles Darwin* (CD114) during August used satellite data and drifting buoys to track the change in physical and biological processes associated with the flow within a filament. Synthetic Aperture Radar (SAR) data were also supplied during this cruise to locate the internal waves for investigation and comparison with measurements using the FLY turbulence probe, though high winds limited the visibility of the internal wave signal.

Figure 1 shows SeaWiFS chlorophyll maps representative of the two legs of the CD114 cruise. Leg 1 was characterised by strong upwelling and high phytoplankton ($> 1 \text{ mg chl. m}^{-3}$) on shelf, with two significant filaments between 42-43°N. One filament is seen to interact with an eddy near 42°N, 10°W, entraining high-chlorophyll water into an anticyclonic spiral. The Lagrangian experiment took place along this filament during leg 2, and experienced both lower biological activity and horizontal currents than expected. The mosaic of chlorophyll maps between 18 and 21 Aug. indicates lower levels of phytoplankton abundance on the shelf and within the filament than during leg 1. The wind plot in Figure 2 shows a major relaxation in upwelling winds at the end of leg 1 (7-10 Aug.) and a minor relaxation during leg 2 (13-17 Aug); this is the probable cause of the lower chlorophyll concentrations near the coast, and reduced flow from the upwelling zone into the filament.

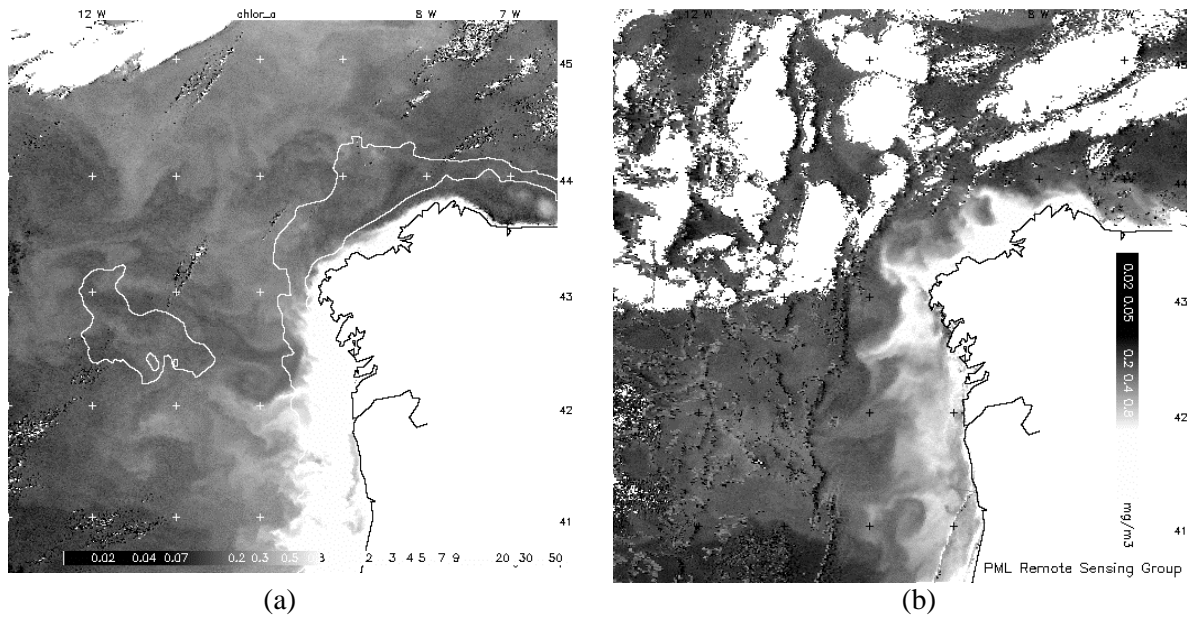


Figure 1. Chlorophyll distribution during *CD114* cruise: (a) Leg 1: 03 Aug. 1998; (b) Leg 2: mosaic of 18-21 Aug. 1998.

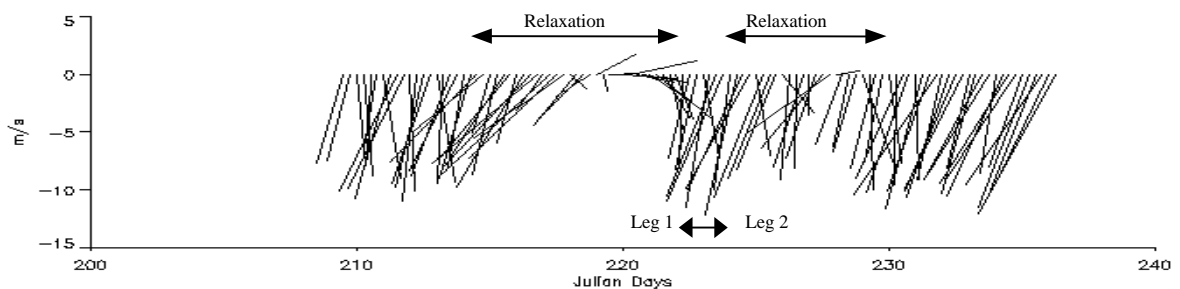


Figure 2. ECMWF wind analysis for OMEX II-II region (42°N, 9°W) 6-hourly through *CD114* cruise period (29 Jul. – 24 Aug. 1998).

Routine processing: Approximately 2000 SST images and 350 ocean colour scenes were processed this year for the OMEX region on the same day as reception, and disseminated over the World-Wide-Web. Unusually, upwelling conditions were sustained by predominantly northerly winds until early December 1998 (Figure 4). The SST for 6th Nov. shows a defined upwelling zone and several small filaments (Figure 3a). The extended upwelling season postponed the formation of the northward ‘Navidad’ current, shown by the tracks of drifters released during *Meteor M43/2* (Barton, Torres, and Miller, 1999).

Figure 3b shows strong upwelling (with $\sim 3 \text{ mg chl m}^{-3}$) and well-developed filaments in a SeaWiFS chlorophyll image from 17 Mar. 1999, several months earlier than expected. The spring bloom normally produces high chlorophyll concentrations near to the coast or in isolated patches.

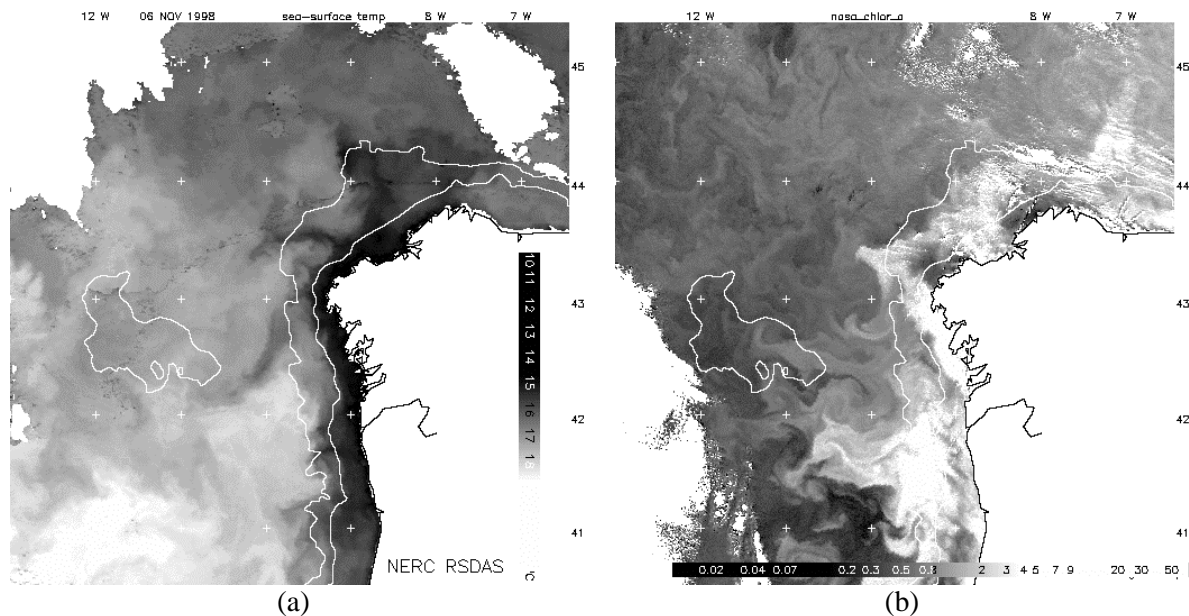


Figure 3. Unusual events this year: (a) SST map from 06 Nov. 1998 indicating winter upwelling; (b) Chlorophyll map from 17 Mar. 1999 showing well-developed filaments.

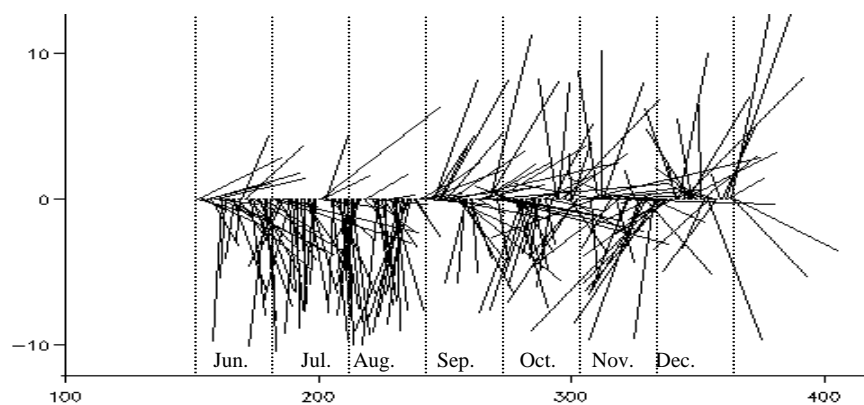


Figure 4. ECMWF wind analysis for OMEX II-II region (42°N, 9°W) daily at 1200 UTC from Jun. to Dec. 1998, showing predominantly northerly winds until early December.

II.1.6 Feature statistics:

Figure 5 presents examples from the data-set of 2,000 composite front maps processed for the Galician region. The density of a contour indicates both the gradient and temporal persistence of a front at that location, thus the darker lines delineate the most significant features observed during the period. The leftmost map is a 6-day composite of chlorophyll ‘fronts’ derived from SeaWiFS scenes acquired during *CD114* leg 1 (2-7 Aug. 1998). The middle map is a 3-day SST front map at the end of leg 2 (22-24 Aug.), and shows many filaments, one of which is being entrained by an anticyclonic eddy near 42°N, 11°W. The final image, from 17-19 Sep. 98, is one of a animated sequence which shows a shelf-water eddy (SWODDY) about to detach from the northern upwelling region.

The automated technique has been validated by comparing the detected fronts against fronts manually annotated on 7 SST and 7 chlorophyll images. On average, 93% of the true temperature fronts and 90% of the chlorophyll fronts were detected, and in both cases the locations were within 2.2 km of the true front. Animations of the cruise periods have been made available on the web site, and statistics on filament and eddy distributions are being derived from the 1993-9 data-set.

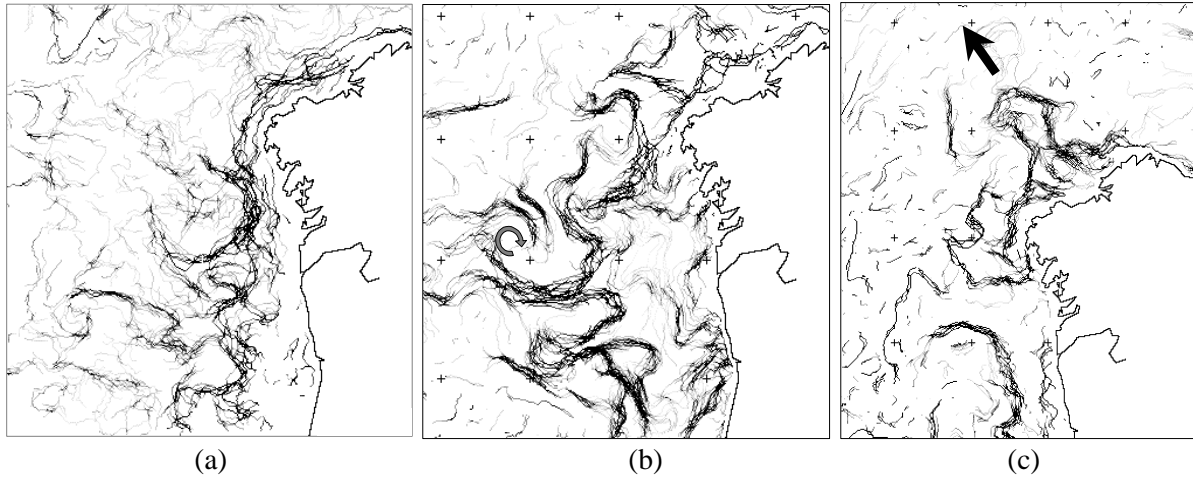


Figure 5. Composite front maps used to improve visualisation of filaments and eddies:
 (a) Chlorophyll fronts 2-7 Aug. 98;
 (b) SST fronts 22-24 Aug. 98, arrow indicates interaction of filament with eddy;
 (c) SST fronts 17-19 Sep. 98 with eddy about to detach from upwelling region.

A time-series of upwelling indices for the Vigo region during OMEX I and II-II has been obtained (Figure 6). The plot indicates the average monthly Ekman offshore transport, in cubic metres per second per 100 metres of coastline. These data appear to relate well to the conditions experienced during the OMEX II-II cruises indicated, such as the low upwelling experienced during Jun. 1997 on *CD105*, and the sustained upwelling of summer 1998 sampled on *CD114*. The extension of upwelling until Dec. 1998 observed in satellite images (Figure 3a) is also represented.

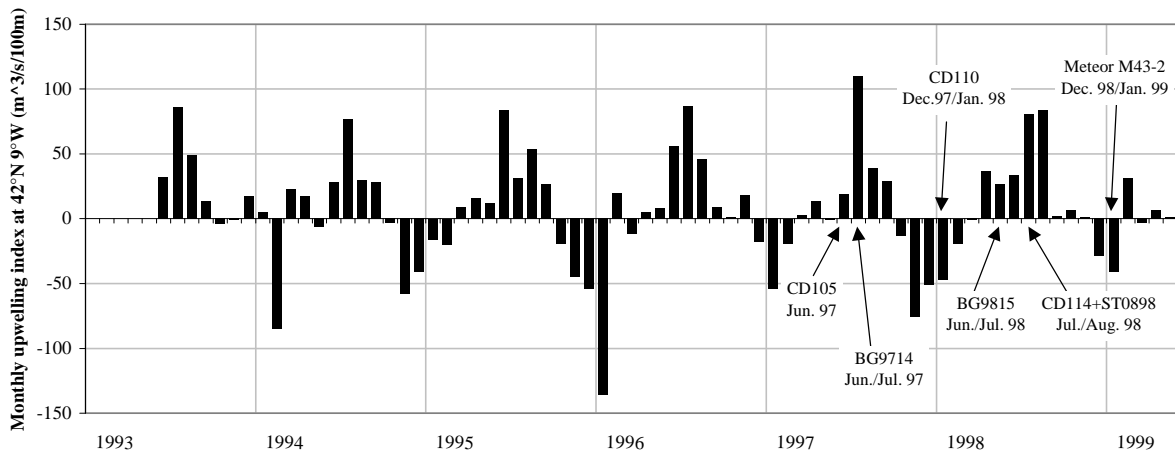


Figure 6. Monthly upwelling index for the Vigo region for the entire OMEX I and II-II period, derived from FNMOC synoptic pressure analyses.

The average seasonal upwelling distribution was derived from the monthly upwelling indices from 1981 to 1999 (Figure 7). Although the mean distribution is as expected, it is interesting to note the large variability in all months – only June to September can be expected to have a net upwelling, whereas all other months include the possibility of a net upwelling or downwelling within 1 standard deviation. In order to resolve the short wind-driven fluctuations in upwelling, during year 3 further upwelling indices based on 6-hourly wind fields will be calculated. These data will be used to set the satellite observations in context, and provide further input to the modelling effort.

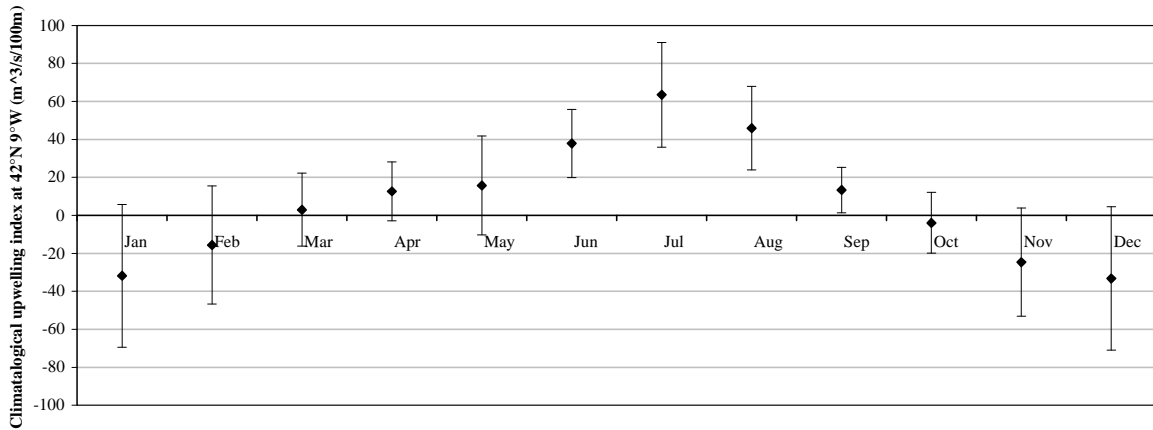


Figure 7. Climatological upwelling index for Vigo region, showing for each month the mean and standard deviation of upwelling indices between 1981 and 1999.

II.12.1 Near-real time cruise support: Individual AVHRR SST and thermal infrared images and SeaWiFS ocean colour images, are being continuously processed in near-real time and disseminated to OMEX scientists via the web site and Inmarsat transmissions. Table 1 lists those cruises supported with near-real time data this year.

Belgica	BG9815	25/06/1998 to 15/07/1998
Prof. Shtockman	ST0898	01/08/1998 to 11/08/1998
Charles Darwin	CD114	29/07/1998 to 24/08/1998
Meteor	M43-2	28/12/1998 to 14/01/1999
Almeida Carvalho	OMEX99	03/05/1999 to 30/05/1999

Table 1. OMEX II-II cruises supported with near-real time remote sensing.

II.12.2 Water-leaving radiance (L_{wn}) comparisons: Figure 8a shows a plot comparing the SeaWiFS measured L_{wn} 490 and the L_{wn} 490 measured using the optical profiling rig. The filled circles represent data collected on the *Belgica* BG9815 cruise and the open circles are match-ups within the SeaWiFS SEABASS data set. Only 4 points taken aboard *Belgica* were eligible for inclusion in SEABASS due to the SeaWiFS protocol requiring data to be within 2 hours of a satellite overpass unobstructed by cloud. However it can be clearly seen that the measurements taken aboard the *Belgica* fit within the expected data spread. This suggests that at 490 nm the atmospheric correction is working correctly. Similar results were obtained for 412, 443, 510 and 555 nm.

Pigment algorithm validation: Figure 8b shows a comparison between the operational SeaWiFS chlorophyll *a* algorithm (OC2V2) applied to values taken from the optical profiler, and *in situ* HPLC chlorophyll *a*. The plot shows that the algorithm consistently overestimates values of chlorophyll *a* at low concentrations ($< 1 \text{ mg m}^{-3}$) and underestimates at high concentrations ($> 1 \text{ mg m}^{-3}$). The slope of the relationship shows that, overall, the algorithm is underestimating the value of chlorophyll *a*.

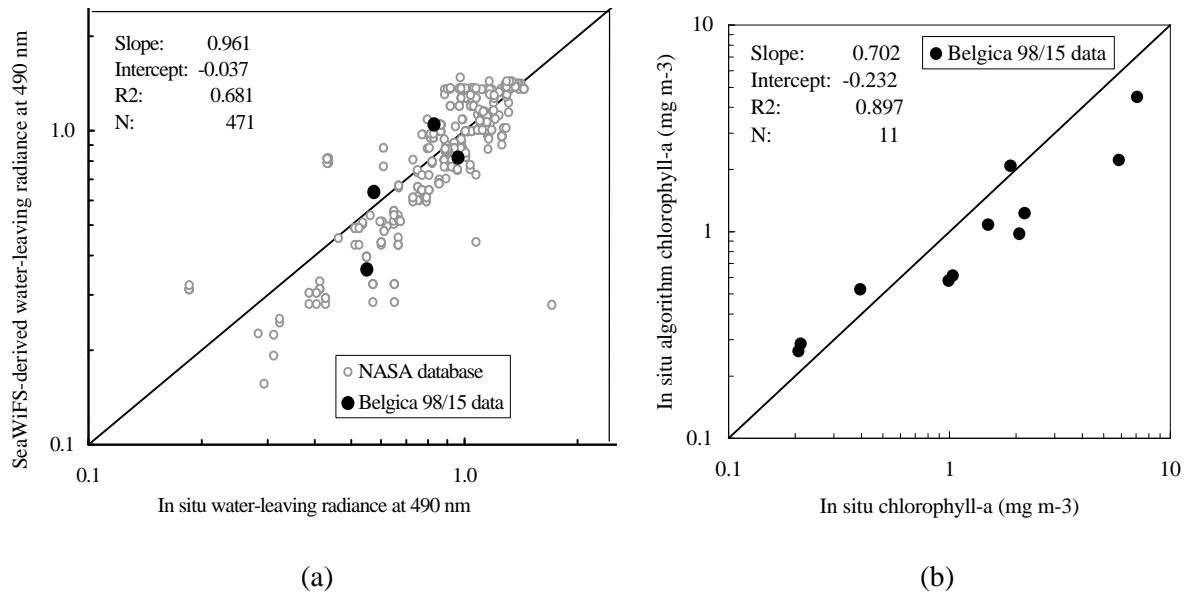


Figure 8. Comparisons between (a) SeaWiFS-measured and *in situ* water-leaving radiance at 490 nm; (b) chlorophyll *a* estimated *in situ* radiance, and that measured *in situ* using HPLC.

Chlorophyll algorithms: The most important variable in algorithms to retrieve primary production from satellite is the chlorophyll *a* concentration (Behrenfeld and Falkowski, 1997). HPLC data provided by PML-a were used to validate chl-*a* pigment algorithms using latest version of SeaWiFS data. The 12 hour comparisons gave $C_{\text{sat}} = 0.73 C_{\text{HPLC}} + 0.35$, $R^2 = 0.73$, $n = 16$) and the <2 hour comparisons (Figure 9), $C_{\text{sat}} = 0.81 C_{\text{HPLC}} + 0.28$, $R^2 = 0.87$, $n = 8$. In both cases SeaWiFS underestimated chlorophyll at higher values and overestimated at lower values (*i.e.*, retrieval slopes < 1.0) with, not surprisingly, a better R^2 for the <2 hour comparison.

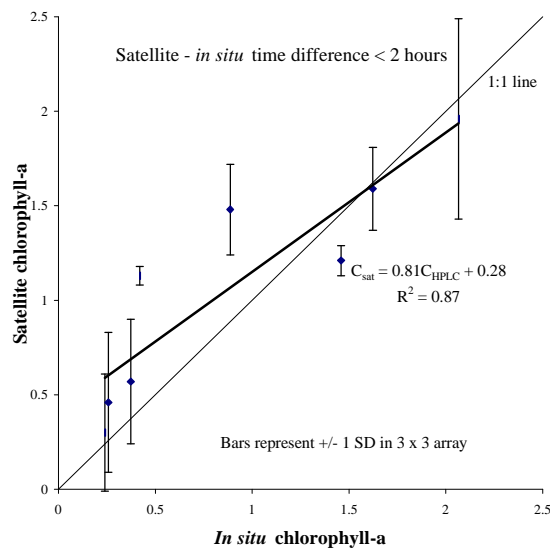


Figure 9. Validation of SeaWiFS chlorophyll algorithms using *CD114* data.

Optical measurements comprising upwelling radiance and downwelling irradiance at five wavelengths coincident with SeaWiFS were taken on *Belgica BG9815* (see above). A comparison of *in situ* and SeaWiFS retrieved radiances did not reveal biases. However, a comparison of HPLC chlorophyll and chlorophyll calculated from the *in situ* radiances and the SeaWiFS operational algorithm (OC2v2) gave a regression $\ln C_{\text{OC2v2}} = 0.70 \ln C_{\text{HPLC}} - 0.23$, $R^2 = 0.90$ (Figure 8b). This suggests that the

problem with chlorophyll retrievals lies with the algorithm not the SeaWiFS atmospheric correction. It is planned to reprocess the SeaWiFS images obtained during *CD114* a third time using the algorithm constructed on-board *Belgica* and compared with *CD114* HPLC providing an independent test.

Production algorithms: A regression of primary production (from ^{14}C incubations) integrated to the 1% light level against surface chlorophyll *a* resulted in 86% of variance explained and 88% in log-transformed variables (Figure 10a). The explanation of variance is much higher than previous experiments and data compilations (*e.g.*, Behrenfeld and Falkowski, 1997) albeit with a small data set ($N=10$). Comparison with a similar analysis in OMEX I for the Goban Spur reveals a similar slope (0.61 *cf.* 0.55 in OMEX I) but a higher intercept (*i.e.*, higher production for a given level of chlorophyll in OMEX II-II). This may be due to the higher temperature, higher light levels in the more southerly OMEX II-II site; this, and other factors, will be investigated in year 3. There will also be an investigation of more complex semi-analytical production algorithms that require additional parameters obtained on *CD114*.

SST-Nitrate algorithms:

Figure 16b shows the *CD114* nitrate vs. temperature for all CTD casts in leg b (but excluding the along track data). The nitrate decreases with increasing temperature, and beyond $\sim 16^\circ\text{C}$ is essentially undetectable. Individual CTD's show little scatter and so the mechanism for applying the algorithms to large area satellite images needs to be considered. Interestingly, the variation of NO_3 with temperature below 16°C appears linear implying the processes of nitrate uptake and temperature increase occur at the same rate (Minas and Codispoti, 1993).

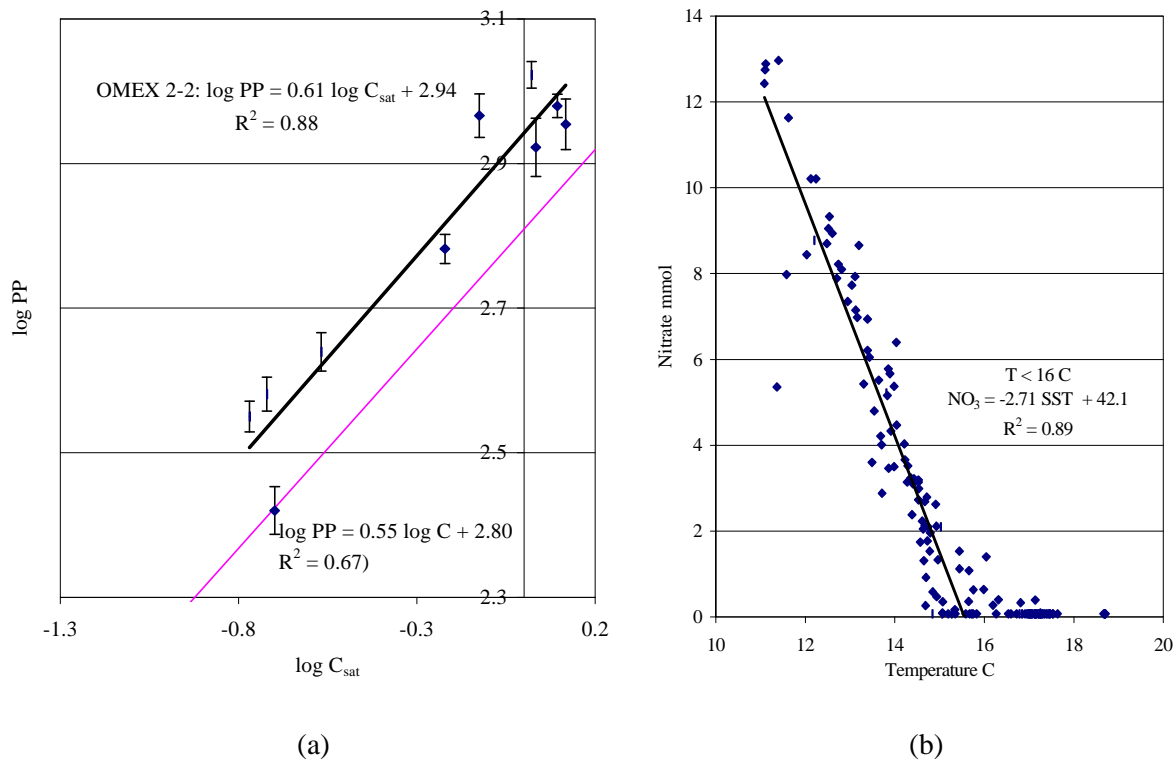


Figure 10. (a) Remote sensing retrieval of total primary production based on SeaWiFS chlorophyll concentration, using *CD114 in situ* data. (b) Relationship between *in situ* temperature and nitrate on *CD114*.

Discussion

This year the Remote Sensing Group has processed 2000 SST and 350 ocean colour scenes for the OMEXII region of interest. The near-real time acquisition and processing of this data has allowed the successful and, in some cases, essential support of five OMEX cruises. Apart from this operational aspect, this year has seen research, development and validation of SeaWiFS algorithms, SST-nitrate

relationships and front detection. The optical measurements taken aboard the *Belgica BG9815* cruise, from which water leaving radiances were derived, show excellent agreement with the global NASA database, implying that the SeaWiFS atmospheric correction procedure is working correctly. However, the HPLC-derived chlorophyll *a* comparison shows a departure from the current operational SeaWiFS algorithm when it is applied to the *in situ* optical measurements, the ratio of algorithm to HPLC-derived chlorophyll *a* being 0.702. This is close to the result obtained when the satellite estimates were compared with HPLC derived chlorophyll *a*, the ratio in this case being 0.81. This suggests that the operational SeaWiFS algorithm requires improvement in such regions with moderate to high values of chlorophyll *a*. The SST-Nitrate algorithms were derived from *CD114* data with a view to being able to remotely sense the new (or nitrate-driven) production. The automated front detection technique has been further developed in terms of visualisation and statistical validation. Statistics of the OMEX II-II upwelling season between 1981 and 1999 show that a net upwelling is possible during any month of the year but that the summer season (June, July and August) is characterised solely by upwelling. June until early December 1998 was dominated by winds from a northerly quadrant that forced a strong and extended upwelling season throughout the summer and autumn months.

Acknowledgements

We wish to thank Sam Lavender (PML) for all aspects of SeaWiFS data processing, NERC Dundee Satellite Receiving Station for the acquisition of satellite data, NASA and Orbimage for providing SeaWiFS data, NOAA Pacific Fisheries Environmental Laboratory for supplying upwelling indices, and BADC for the ECMWF operational and re-analysis data.

References

- Barton E.D., Torres R., Miller P.I., 1999, Summer and winter Lagrangian flows over the Iberian continental margin. OMEX II-II Second Annual Workshop, Plymouth, April 1999.
- Behrenfeld M.J., and P.G. Falkowski, (1997) A consumers guide to phytoplankton primary productivity models, *Limnol. Oceanogr.*, 42, 1479-1491.
- Cayula, J.-F., and Cornillon, P., 1992, Edge detection algorithm for SST images. *Journal of Atmospheric and Oceanic Technology*, 9, 67-80.
- Joint, I., Wollast, R., Chou, L., et al., 1997, Pelagic production at the Celtic Sea shelf break – the OMEX I project. *Deep Sea Research* (in press).
- Lavender, S.J. and Groom, S.B., 1998, The SeaWiFS Automatic Data Processing System (SeaAPS). *International Journal of Remote Sensing*, (submitted).
- Miller, P., Groom, S., McManus, A., Selley, J., and Mironnet, N., 1997, PANORAMA: a semi-automated AVHRR and CZCS system for observation of coastal and ocean processes. *RSS97: Observations and Interactions, Proceedings of the Remote Sensing Society*, pp. 539-544, Reading, September 1997.
- Miller, P., Groom, S., McManus, A., Selley, J., Mironnet, N., and Lavender, S., Panorama: an automated AVHRR, CZCS and SeaWiFS system for monitoring oceanic processes. *International Journal of Remote Sensing*, (submitted).
- Minas H.J., and L.A. Codispoti (1993), Estimation of primary production by observation of changes in the mesoscale nitrate field, *ICES Mar. Sci. Symp.*, 197, 215-235.
- Sathyendranath S., T. Platt, E.P.W. Horne, W.G. Harrison, O. Ulloa, R. Outerbridge, and N. Hoepffner, (1991). Estimation of new production in the ocean by compound remote sensing. *Nature*, 353, 129-133.
- Schwing F.B., O'Farrell M., Steger J., Baltz K., 1996, Coastal upwelling indices, West Coast of North America 1946-1995, *NOAA Technical Memorandum NMFS-SWFSC-231*, 207 pp.